Nano Research
2023, 16(4): 5511–5516
ISSN 1998-0124 CN 11-5974/O4
https://doi.org/10.1007/s12274-022-5106-8

Research Article

On the voltage sweep behavior of quantum dot light-emitting diode

Xiangwei Qu[1,2,§], Jingrui Ma[1,2,§], Pai Liu[1,2], Kai Wang[1,2], and Xiao Wei Sun[1,2] (✉)

[1] *Institute of Nanoscience and Applications, Southern University of Science and Technology, Shenzhen 518055, China*
[2] *Key Laboratory of Energy Conversion and Storage Technologies (Southern University of Science and Technology), Ministry of Education, Guangdong University Key Laboratory for Advanced Quantum Dot Displays and Lighting, Guangdong-Hong Kong-Macao Joint Laboratory for Photonic-Thermal-Electrical Energy Materials and Devices, Shenzhen Key Laboratory for Advanced Quantum Dot Displays and Lighting, and Department of Electrical and Electronic Engineering, Southern University of Science and Technology, Shenzhen 518055, China*
[§] *Xiangwei Qu and Jingrui Ma contributed equally to this work.*

© Tsinghua University Press 2022, corrected publication 2023.
Received: 5 August 2022 / **Revised:** 4 September 2022 / **Accepted:** 26 September 2022

ABSTRACT

The origin of the efficiency drop of quantum dot light-emitting diode (QLED) under consecutive voltage sweeps is still a puzzle. In this work, we report the voltage sweep behavior of QLED. We observed the efficiency drop of red QLED with ZnMgO electron transport layer (ETL) under consecutive voltage sweeps. In contrast, the efficiency increases for ZnO ETL device. By analyzing the electrical characteristics of both devices and surface traps of ZnMgO and ZnO nanoparticles, we found the efficiency drop of ZnMgO device is related to the hole leakage mediated by trap state on ZnMgO nanoparticles. For ZnO device, the efficiency raise is due to suppressed electron leakage. The hole leakage also causes rapid lifetime degradation of ZnMgO device. However, the efficiency and lifetime degradation of ZnMgO device can be eliminated with shelf aging. Our work reveals the distinct voltage sweep behavior of QLED based on different ETLs and may help to understand the lifetime degradation mechanism in QLED.

KEYWORDS

quantum dot light-emitting diode, voltage sweep behavior, efficiency drop, hole leakage current

1 Introduction

Quantum dot light-emitting diode (QLED) featuring self-emission and narrow linewidth is highly attractive for next generation displays [1–5]. It enjoys a better contrast ratio and wider color gamut compared to existing displays including organic light-emitting diode (OLED) and liquid crystal display (LCD). Since its first report, the performance of QLED has been boosted with extensive efforts [1–5]. At present, the maximum external quantum efficiency (EQE) of red, green and blue QLEDs has reached 21.6%, 28.7% and 21.9% respectively [2, 3]. Furthermore, the operation lifetime T_{95} of red, green, and blue QLEDs has reached 7,668, 7,500 and 57 h at 1,000 cd/m^2, respectively [3, 4]. In particular, the operation lifetime T_{50} of inkjet-printed red and green QLEDs has reached 25,178 and 20,655 h at 1,000 cd/m^2 [5], which satisfy the requirement of display applications.

QLEDs are self-emitting devices, consisting of an emissive QD layer between electron transport layer (ETL) and hole transport layer (HTL), and two electrodes [6]. For a working device, electrons and holes are injected from their respective electrode under bias, and transport through charge transport layer, then they are injected into QD emission layer to form excitons. After exciton radiative recombination, photons would be generated and then extracted from the device. In a working QLED, the device efficiency EQE = $\eta_r\eta_{PL}\eta_{ex}$ [6], where η_r is the ratio of injected charges that form excitons in QD layer, η_{PL} is the quantum yield of QD film, η_{ex} is the light extraction efficiency. Therefore, η_r is a key factor determining the QLED efficiency. ZnO nanoparticles are commonly employed as electron transport materials in QLED for their matched conduction band minimum (CBM) and high electron mobility [7]. However, it may cause electron over-injection into HTL [3, 8], which would decrease the factor η_r, lowering the device efficiency. According to previous report, Deng et al. discovered that green and blue QLEDs behave poor performance was mainly due to the electron leakage. They employed a new HTL PF8Cz to suppress the electron leakage, which improves the performance of green and blue QLEDs [3]. Wang et al. observed the trap site in PVK could accept over-injected electrons in blue QLED, and they inserted a ZnSe-based QD interlayer to suppress the electron leakage [9]. Apart from the electron leakage, hole leakage in QLED was also reported. For instance, Chrzanowski et al. reported ZnMgO traps mediated hole leakage in green QLED, they found H_2O could passivate the trap states and block the hole leakage path [10]. Wang et al. found standard QLED based on PEDOT:PSS/TFB suffered from strong hole leakage, and developed a new HTL mTFF to alleviate the hole leakage [11]. Therefore, to fabricate high performance QLED, both electron and hole leakage should be suppressed [3, 8–14].

Furthermore, the leakage current plays a dominating role in QLED stability. For operation stability, the QLED lifetime degradation are often associated with the HTL degradation because of the electron leakage into HTL [3, 8, 15]. On the other hand, shelf stability is also an important point of QLED, positive aging i.e., the current density and efficiency improvement of

Address correspondence to sunxw@sustech.edu.cn

QLED after several days' storage is attributed to suppressed leakage current [16, 17]. Besides the effect of leakage current on efficiency and lifetime of QLED, herein, we focus on the impact of leakage current to the voltage sweep behavior of QLED, which is rarely discussed in previous report. In OLEDs, the current efficiency dropped under consecutive voltage sweeps, because of the charged small molecule induced leakage current [18]. Similarly, the device efficiency drop under consecutive voltage sweeps was also observed in QLED [2, 10]. However, the origin is not clear yet. In this work, we observed the efficiency drop of red QLED with ZnMgO ETL under consecutive voltage sweeps, while surprisingly the efficiency of ZnO device raises. By the analysis of the electrical characteristics of both devices and the surface traps of ZnMgO and ZnO nanoparticles, we attribute the efficiency drop of ZnMgO device to hole leakage mediated by trap state on ZnMgO nanoparticles. For ZnO device, the efficiency raise is ascribed to suppressed electron leakage. Furthermore, the hole leakage also causes rapid lifetime degradation of ZnMgO device. Finally, the EQE and lifetime degradation of ZnMgO device can be eliminated with shelf aging. Our work reveals a perspective of the origin of efficiency and lifetime degradation in red QLED and may help to understand the device physics of QLED.

2 Results and discussion

2.1 Voltage sweep behavior of QLED

Our QLED was fabricated with the following structure: ITO /PEDOT:PSS/TFB/QDs/ZnMgO/Al, where ITO, PEDOT:PSS, TFB, QDs, ZnMgO, Al functions as anode, hole injection layer, hole transport layer, emission layer, electron transport layer and cathode, respectively. The EL spectrum of fabricated QLED is located at 621 nm (Fig. S1 in the Electronic Supplementary Material (ESM)), suggesting a pure red emission of our device. To study the voltage sweep behavior of QLED, five consecutive voltage sweeps are conducted on red QLED with ZnMgO ETL. Each voltage sweep is conducted after the end of previous sweep without any pause, the voltage step is 0.1 V and each voltage sweep lasts for about 20 s. Figure 1(a) shows the current density–voltage (*J*–*V*), luminance–voltage (*L*–*V*), and current efficiency–voltage characteristics of the ZnMgO device. It is clear that the current density of ZnMgO device raises under five consecutive voltage sweeps. For instance, the current density of ZnMgO device at 4 V is 59.52 mA/cm^2 at the first sweep, then it raises to 61.12, 61.96, 62.72, 63.28 mA/cm^2 respectively in the next four voltage sweeps. At the same time, the luminance of ZnMgO device at 4 V increases from 14,526 to 14,918, 15,227, 15,529, and 15,772 cd/m^2 for the 2nd to 5th sweeps, respectively. They are shown in details in Fig. 1(c). However, the maximum current efficiency (CE) of the ZnMgO device in this case drops from 29.52, to 25.80, 25.06, 25.03, 24.96 cd/A (Fig. 1(c)), which is similar to the results in the previous report [2, 10]. To investigate the origin of CE drop in ZnMgO device, we employ ZnO nanoparticles as ETL to fabricate red QLED. As shown in Fig. 1(b), the current density and luminance of ZnO device raise under voltage sweeps, but the maximum CE of ZnO device tends to raise under voltage sweeps. Concretely, the maximum CE of ZnO device raise from 23.02 to 23.69, 24.01, 24.25, and 24.30 cd/A (Fig. 1(c)) for the 2nd to 5th sweeps, respectively. Therefore, although the current density and luminance of both devices are increased under voltage sweeps, their maximum CE exhibits opposite trend in this case. Herein, we aim to figure out the mechanism of the distinct voltage sweep behavior between ZnMgO and ZnO based devices, i.e., i) why the current density and luminance of both devices raise under voltage sweeps; ii) why the maximum CE of ZnMgO device drops under voltage sweeps, while it increases for ZnO device.

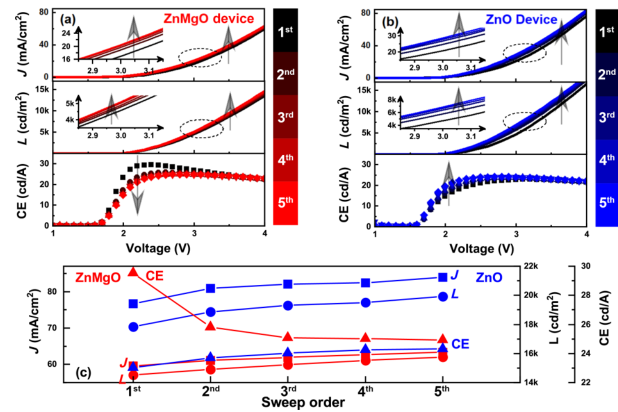

Figure 1 Current density-luminance-current efficiency-voltage characteristics of (a) ZnMgO and (b) ZnO devices under five consecutive voltage sweeps. The insets show the corresponding enlarged detail in (a) and (b). (c) Current density and luminance @ 4 V, and maximum CE versus sweep order of ZnMgO and ZnO devices.

2.2 Electrical analysis of QLED with different ETL

The increase of QLED current density under voltage sweeps may come from conductivity improvement of the ZnMgO and ZnO films. As we know, ZnO is widely employed in resistive switching memory device for their tunable resistance under electric field [19–23]. Usually, ZnO exhibiting high resistance state (HRS) will turn to low resistance state (LRS) under a positive voltage sweep [19]. For instance, Chen et al. argued that oxygen ion migration under electrical field forms conducting channel [20], which improve the conductivity of ZnO. Besides, Chang et al. concluded that an interfacial metal oxide layer forms at the metal/ZnO interface, which controls the oxygen outflow and leads the resistive switching process [21]. Therefore, ZnO exhibits clear resistive switching effect under electrical field. Figure 2(a) shows the current density–voltage characteristics of the devices with the following structures: ITO/ZnMgO/Al and ITO/ZnO/Al. The *J*–*V* characteristics of both devices show evident hysteresis. Concretely, it exhibits HRS in forward sweep and LRS in reverse sweep for both devices, indicating that conductivity of ZnO and ZnMgO nanoparticle films are improved under the electric field. Therefore, the current density and the corresponding luminance increase for both ZnO and ZnMgO devices under consecutive voltage sweeps.

In a working QLED, the current efficiency CE = *L*/*J*. Therefore, although the current density and luminance of ZnMgO device raise at the same time under the consecutive voltage sweeps, to explore the origin of EQE drop in ZnMgO device, we have to consider the ratios of the current density and luminance for 2nd to 5th sweeps (Figs. S2 and S3 in the ESM) with respect to that in first sweep i.e., J_2/J_1, J_3/J_1, J_4/J_1, J_5/J_1 and L_2/L_1, L_3/L_1, L_4/L_1, L_5/L_1. We take J_5/J_1 and L_5/L_1 as an example, as shown in Fig. 2(b), the current density increment is larger than the luminance increment of ZnMgO device ($J_5/J_1 > L_5/L_1$). For instance, J_5/J_1 is 2.38 at the applied bias of 1.7 V, which is larger than L_5/L_1 (2.07). That is to say, the luminance increment cannot follow the current density increment, then part of current may leak out and doesn't contribute to luminance increase, which causes the CE drop in ZnMgO device. To identify the leakage current cause of the CE drop, we analyze the luminance-current density characteristics of ZnMgO device (Fig. S4(a) in the ESM). With the same current density, the luminance drops under voltage sweeps, indicating part of current leaks out that doesn't contribute to the emission. Furthermore, the peak capacitance of ZnMgO device drops slightly from 3.69 to 3.63 nF under voltage sweeps (Fig. 2(c)), suggesting the charge leakage in ZnMgO device. On the other hand, the voltage for the minimum CE (0.611) is 1.9 V, where the

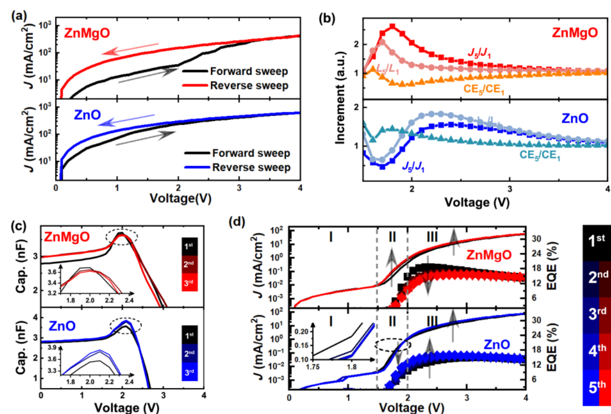

Figure 2 (a) Current density-voltage characteristics of ITO/ZnMgO/Al or ITO/ZnO/Al in forward and backward sweep, (b) current density increment (J_5/J_1), luminance increment (L_5/L_1), and current efficiency increment (CE_5/CE_1) of ZnMgO and ZnO devices, (c) capacitance-voltage characteristics of ZnMgO and ZnO devices with a frequency of 1 kHz, (d) current density-EQE-voltage characteristics of ZnMgO and ZnO devices. The inset shows the enlarged detail of the curves.

ratio of L_5/L_1 over J_5/J_1 reach its minimum. Such an applied bias is indeed located at leakage current regions [17, 24], implying the CE drop of ZnMgO device is attributed to the leakage current.

For ZnO device, the case is more complex. Shown in Fig. 2(b) is the current density (J_5/J_1), luminance (L_5/L_1), and current efficiency (CE_5/CE_1) ratios of ZnO device. The luminance and current density drop before 1.9 V and raise after 2 V under voltage sweeps, which are quite different from that of ZnMgO device. Moreover, the applied bias at the maximum CE ratio of ZnO device is 1.8 V, in this case, the luminance and current density drop simultaneously. However, L_5/L_1 is larger than J_5/J_1, i.e., although the current density of ZnO device drops, but the luminescence efficiency is improved, which contributes to the CE raise. In the capacitance–voltage (C–V) characteristics of ZnO device (Fig. 2(c)), the peak capacitance of ZnO device raises slightly from 3.57 to 3.85 nF under voltage sweep, implying the electron accumulation in ZnO device under voltage sweep [8]. According to previous report, charge injection can be modulated by the electron in QD layer under electrical aging [25]. Therefore, electrons left in first voltage sweep can block the electron over-injection in next voltage sweep owing to the Coulombic interaction, which suppresses electron leakage in ZnO device, thereby causing the current density drop before 1.9 V. On the other hand, the factor η_r (the ratio of injected charges that form excitons in QD layer) is improved with suppressed electron leakage, which in turn improve the luminescence efficiency. Figure S4(b) in the ESM show the luminance-current density characteristics of ZnO device, With the same current density, the luminance raises under voltage sweeps, suggesting higher luminescence efficiency at 2nd to 5th sweeps in ZnO device.

Therefore, we can understand the opposite CE trend of ZnMgO and ZnO devices combining with J–L–C–V characteristics. As shown in Fig. 2(d), we separate the J–V curve (log scale) of ZnMgO and ZnO devices into three regions. The current density of both devices keeps unchanged in Region I and raises in region III under voltage sweep, while the J–V characteristics of ZnMgO and ZnO devices is quite distinct in region II. For ZnMgO device, the leakage current in region II raise under voltage sweeps, then factor η_r would decrease in this case, which lower the device efficiency. The maximum EQE of ZnMgO device drops from 18.57% to 15.68%. Furthermore, the voltage at the maximum EQE is increased from 2.4 to 2.9 V, indicating the charge balance in ZnMgO device is weakened by the leakage current. For ZnO device, the leakage current in region II drops under voltage sweeps. As discussed above, accumulated electron in ZnO device can block electron over-injection, which suppresses the electron leakage in ZnO device. Then the factor η_r would raise with suppressed leakage current, which improves the device efficiency. The maximum EQE of ZnO device raise from 15.05% to 15.88% in this case. Furthermore, the voltage at the maximum EQE is decreased from 3.1 to 2.7 V, which also have the opposite trend to ZnMgO device, suggesting a more balanced charge injection under voltage sweeps in ZnO device [17]. Therefore, the EQE drop of ZnMgO device is attributed to leakage current, and the EQE raise of ZnO device is ascribed to suppressed electron leakage.

2.3 The origin of hole leakage

Besides the origin of EQE drop of ZnMgO device, we also investigate the source of the leakage current in ZnMgO device. According to previous report, the ZnMgO nanoparticles can be embedded in red QD layer, which provide a hole leakage channel across the QD layer [10, 17]. Owing to the energy alignment of highest occupied molecular orbital (HOMO) of TFB and the trap state of ZnMgO, hole can be transferred from TFB to ZnMgO layer through the embedded ZnMgO nanoparticles, which forms a hole leakage path. Therefore, the hole leakage should be highly correlated to the surface traps in ZnMgO nanoparticles. Considering the suppressed electron leakage in ZnO device, it is necessary to compare surface traps of ZnO and ZnMgO nanoparticle films. We measured the PL spectra of ZnO and ZnMgO nanoparticle films (thickness ~50 nm). As shown in Fig. 3(a), apart from an intrinsic emission, a strong green-yellow band is also observed in PL spectra of ZnO and ZnMgO nanoparticle films, which is associated with oxygen defects [26]. The defect emission of ZnO and ZnMgO films peak at 538 and 508 nm, respectively. It is clear that the defect emission intensity of ZnMgO film is stronger than that of ZnO film, indicating the defect density of ZnMgO film is higher than ZnO film. To quantitatively compare the defects of ZnO and ZnMgO films, XPS was conducted to analyze the surface oxygen composition. As shown in Figs. 3(b) and 3(c), the O 1s was deconvoluted into two peaks using Gaussian fitting. One peak is located at 530.1 eV, representing the oxygen lattice, while another peak is located at 531.4 eV, representing the oxygen vacancy and hydroxyl groups,

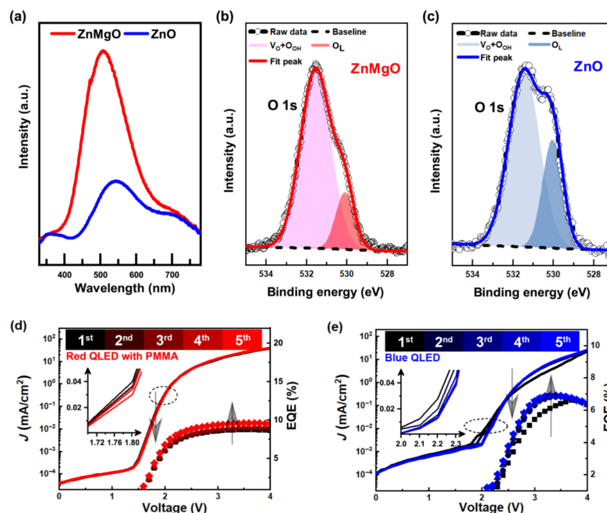

Figure 3 (a) PL spectra of ZnO and ZnMgO films, XPS spectra of (b) ZnMgO and (c) ZnO films on O 1s, (d) current density-EQE-voltage characteristics of red QLED with PMMA interlayer under consecutive voltage sweeps, (e) current density-EQE-voltage characteristics of blue QLED with ZnMgO ETL under consecutive voltage sweeps. The inset shows the corresponding enlarged detail of curves.

which is regarded as oxygen defect [17]. The ratio of oxygen defects over oxygen lattice of ZnO film is 2.5, however, it raises to 5.1 for ZnMgO film (Table S1 in the ESM), implying the trap density of ZnMgO film is much higher than that of ZnO film. Therefore, the leakage current in ZnMgO device is attributed to hole leakage mediated by trap state in ZnMgO nanoparticles, which is illustrated in Fig. 4(a). For ZnO device, the hole leakage path is blocked in ZnO device because of lower trap density. Instead, the accumulated electrons in QD layer play a dominating role to suppress electron leakage, which is illustrated in Fig. 4(b).

The surface trap difference between ZnO and ZnMgO films provide a reasonable explanation for hole leakage path in ZnMgO device, but we still can't prove it directly. To verify the source of hole leakage, we insert a polymer PMMA interlayer between the red QD layer and ZnMgO layer to prevent the ZnMgO nanoparticle from embedding into QD layer. As shown in Fig. 3(d), the leakage current of red QLED drops slightly under voltage sweeps, suggesting suppressed hole leakage by PMMA interlayer, which is illustrated in Fig. 4(c). Then the EQE of QLED consequently raises under voltage sweeps, which reveals the source of hole leakage. Furthermore, we compare the performance of blue QLED with ZnMgO ETL. Owing to the quantum size effect [27, 28], the size of blue QD is smaller than that of red QD, shown in Fig. S6 in the ESM is the TEM images of red QD and blue QD, the diameter of red QD is about 13 nm, while it is only 6 nm for blue QD. Considering the diameter of ZnMgO nanoparticle is about 5 nm (Fig. S7 in the ESM), the ZnMgO nanoparticle can be embedded into red QD rather than blue QD, which also block the hole leakage path in blue QLED (illustrated in Fig. 4(d)). As expected, the leakage current of blue QLEDs with ZnMgO ETL drops under voltage sweeps (Fig. 3(e)), in this case, the EQE of blue QLED raises from 6.60% to 6.91% with suppressed leakage current. Therefore, the EQE drop of ZnMgO device is indeed attributed to hole leakage.

2.4 Operation lifetime of QLED

Interestingly, the EQE drop of ZnMgO device can be eliminated with shelf aging. Positive aging, i.e., the device efficiency of QLED improvement after several day's storage is frequently reported [16, 17, 29, 30]. Chen et al. contributed the efficiency raise to the interaction between ZnMgO nanoparticles and encapsulation resin, which improved the conductivity of ETL and passivated the trap sites in ZnMgO nanoparticles [16, 17]. Remarkably, in our experiment, the EQE drop of ZnMgO device can be eliminated with shelf aging. As shown in Fig. 5(a), the leakage current of shelf-aged ZnMgO device drops under voltage sweeps, because the trap sites on ZnMgO nanoparticles are passivated by resin with shelf aging [17], which block the hole leakage path. Instead, the accumulated electrons play a dominating role in the current density of shelf-aged ZnMgO device, which suppress the electron leakage. Herein, we should notice that the luminance of shelf-aged ZnMgO device also drops in this case, but the luminance decrement is smaller than the current density decrement (Fig. S9 in the ESM), i.e., the luminescence efficiency of shelf-aged ZnMgO device is improved under voltage sweep. Therefore, the maximum EQE of shelf-aged ZnMgO device raise from 20.71% to 22.58% under voltage sweeps. The current density and luminance of shelf-aged ZnMgO device at 4 V are more than twice higher than that of pristine ZnMgO device. Moreover, the maximum EQE of shelf-aged ZnMgO device are improved from 18.57% to 22.58%, indicating an evident positive aging effect in red QLED. For ZnO device, the maximum EQE raise from 15.88% to 19.53% with shelf aging (Fig. S10 in the ESM).

Apart from the efficiency drop of ZnMgO device, hole leakage also causes rapid lifetime degradation in ZnMgO device. As shown in Fig. 5(b), T_{50} of ZnMgO device is just 6.6 h (at 10,000 cd/m^2) with a constant current of 1.97 mA. As a comparison, the T_{50} of ZnO device is 171 h (at 10,000 cd/m^2) with a constant current of 2.04 mA, exhibiting much longer lifetime for ZnO device. The large gap between the lifetime of ZnMgO and ZnO device is due to continuous luminance drop (Fig. S4(a) in the ESM) in ZnMgO device under electrical aging. That is to say, the hole leakage also plays a dominating role in the lifetime of ZnMgO device. Notably, the operation lifetime of ZnMgO is improved greatly with shelf aging, As shown in Fig. 5(c), the T_{50} of shelf-aged ZnMgO device is 202 h at 10,000 cd/m^2, which is much larger than that of pristine ZnMgO device. The improved lifetime of ZnMgO device is attributed to suppressed leakage current with shelf aging. As shown in Fig. 5(d), the leakage current of shelf-aged ZnO device drops slightly compared to that of pristine ZnO device, but the leakage current of shelf-aged ZnMgO device is much smaller than that of pristine ZnMgO device. For instance, the current density of shelf-aged ZnMgO device at 1.5 V is 0.0011 mA/cm^2, which is one order smaller than that of pristine ZnMgO device (0.0178 mA/cm^2). As discussed above, for shelf-aged ZnMgO device, the hole leakage path is blocked with shelf aging, which suppresses continuous luminance drop. The T_{50} of aged ZnO device is about 523 h at 10,000 cd/m^2, if we take the accelerate factor n = 1.8, the T_{50} of aged ZnO device at 100 cd/m^2 is estimated to be 2,082,000 h.

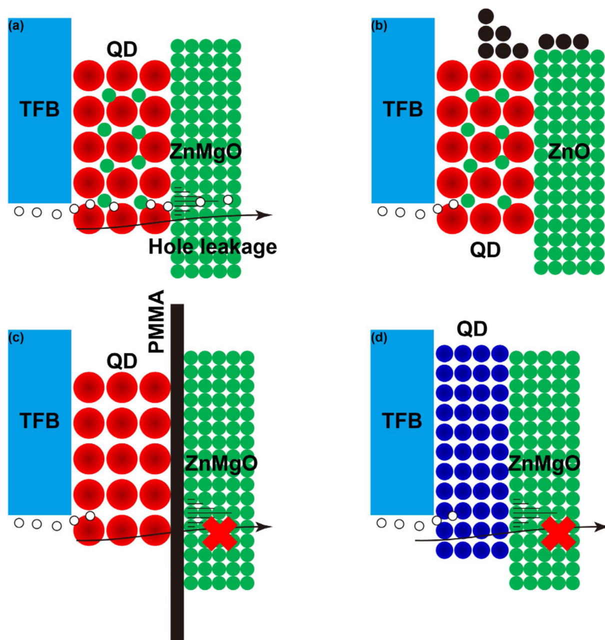

Figure 4 Diagrams of (a) hole leakage path in red QLED with ZnMgO ETL, (b) electron accumulation in red QLED with ZnO ETL, (c) hole leakage path is blocked with a PMMA interlayer, (d) hole leakage path is blocked in blue QLED.

3 Conclusion

In this paper, we studied the voltage sweep behavior of QLED. Distinct difference of QLEDs with ZnMgO and ZnO ETL under voltage sweeps was observed in our experiment; the EQE of ZnMgO device drops continuously, while it raises for ZnO device. By analyzing the electrical properties of both devices and comparing the surface trap of ZnMgO and ZnO nanoparticle films, we found there is a hole leakage in ZnMgO device causing the difference. There is also a distinct lifetime difference between the two devices. However, the EQE and lifetime degradation of ZnMgO device can be eliminated with shelf aging. Our work

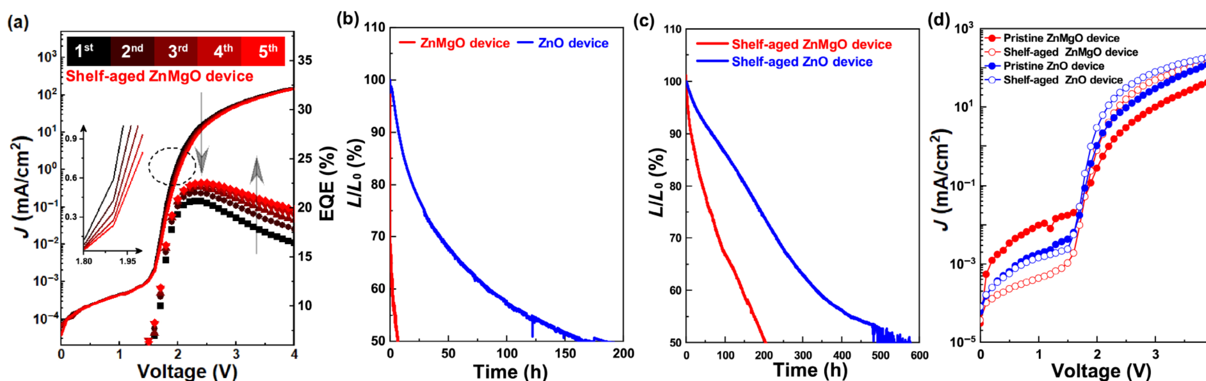

Figure 5 (a) Current density-EQE-voltage characteristics of shelf-aged ZnMgO device, (b) operation lifetime of pristine ZnMgO and ZnO devices, (c) operation lifetime of shelf-aged ZnMgO and ZnO devices, and (d) current density of pristine and shelf-aged ZnMgO devices, pristine and shelf-aged ZnO devices. The inset shows the enlarged detail of curves.

shows the distinct voltage sweep behavior of QLED based on different ETL and may help to understand the device physics in QLED.

4 Method

4.1 Materials

Colloidal ZnO nanoparticles were synthesized according to previously reported method [4]. To synthesize ZnMgO nanoparticles, 15% mole ratio $Mg(CH_3COO)_2·4H_2O$ was added to solvent, the rest processes followed those in ZnO synthesis. Red and blue CdSe/ZnS quantum dots were purchased from Suzhou Xingshuo Nanotech Co., Ltd. TFB was purchased from America Dyes Source. All reagents were used as received without further purification.

4.2 Device fabrication

The ITO glass was cleaned with toluene, acetone, deionized water, and isopropanol under ultrasonication successively for 10 min each, followed by ultraviolet (UV) light treatment for 10 min before use. PEDOT:PSS (Baytron PVP Al 4083, filtered through a 0.45 mm filter) were spin-coated onto ITO glass at 4,000 r.p.m for 45 s and baked at 130 °C for 15 min, then TFB (dissolve in chlorobenzene, 8 mg/mL), red QDs (dissolve in octane,15 mg/mL) were subsequently spin-coated layer by layer at 3,000 r.p.m for 45 s, wherein TFB layer was baked at 120 °C for 15 min, and red QDs layer was baked at 100 °C for 5 min. ZnO or ZnMgO nanoparticles (dissolve in ethanol, 20 mg/mL) was spin-coated at 3,000 r.p.m for 45 s, ZnO or ZnMgO nanoparticles layer was baked at 80 °C for 20 min, after that, the device was transferred into vacuum chamber, and Al (100 nm) electrodes were deposited on the device under a vacuum level of 5×10^{-4} Torr with a speed of 0.5–1 nm/s. The active area of the device was 0.04 cm^2. For red QLED with PMMA device, PMMA (dissolved in dioxane, 3 mg/mL) was spin-coated at 3,000 r.p.m for 45 s and baked at 100 °C for 5 min. For blue QLED, blue QDs (dissolve in octane,10 mg/mL) were spin-coated at 3,000 r.p.m for 45 s and baked at 100 °C for 5 min.

4.3 Characteristics

The electroluminescence (EL) spectra of QLEDs were measured using a fiber optic spectrometer (Ocean Optics USB 2000). The current density–luminance–voltage (J–V–L) characteristics of QLEDs were measured by a dual-channel Keithley 2614B source measure unit and a PIN-25D silicon photodiode. Capacitance–voltage characteristics of QLEDs were determined by Fluxim-paios System. The operational lifetimes of QLEDs were measured by using an ageing system with an embedded photodiode designed by Guangzhou New Vision Opto-Electronic Technology Co., Ltd. The PL spectra of the samples were measured by an Edinburgh Instruments FLS980 spectrometer. XPS spectra were conducted using PHI5000 Versa Probe III.

Acknowledgements

This work was supported by Key-Area Research and Development Program of Guangdong Province (Nos. 2019B010925001 and 2019B010924001), Guangdong University Key Laboratory for Advanced Quantum Dot Displays and Lighting (No. 2017KSYS007).

Electronic Supplementary Material: Supplementary material (device structure, J and L increment of ZnMgO and ZnO devices, L–J characteristics of ZnMgO and ZnO devices, TEM images of red, blue QDs, ZnMgO and ZnO nanoparticles, operation voltage of ZnMgO and ZnO devices, O composition of ZnMgO and ZnO nanoparticles, operation lifetime of reported QLEDs) is available in the online version of this article at https://doi.org/10.1007/s12274-022-5106-8.

References

[1] Dai, X. L.; Zhang, Z. X.; Jin, Y. Z.; Niu, Y.; Cao, H. J.; Liang, X. Y.; Chen, L. W.; Wang, J. P.; Peng, X. G. Solution-processed, high-performance light-emitting diodes based on quantum dots. *Nature* **2014**, *515*, 96–99.

[2] Shen, H. B.; Gao, Q.; Zhang, Y. B.; Lin, Y.; Lin, Q. L.; Li, Z. H.; Chen, L.; Zeng, Z. P.; Li, X. G.; Jia, Y. et al. Visible quantum dot light-emitting diodes with simultaneous high brightness and efficiency. *Nat. Photonics* **2019**, *13*, 192–197.

[3] Deng, Y. Z.; Peng, F.; Lu, Y.; Zhu, X. T.; Jin, W. X.; Qiu, J.; Dong, J. W.; Hao, Y. L.; Di, D. W.; Gao, Y. et al. Solution-processed green and blue quantum-dot light-emitting diodes with eliminated charge leakage. *Nat. Photonics* **2022**, *16*, 505–511.

[4] Liu, D. Q.; Cao, S.; Wang, S. Y.; Wang, H. Q.; Dai, W.; Zou, B. S.; Zhao, J. L.; Wang, Y. J. Highly stable red quantum dot light-emitting diodes with long T_{95} operation lifetimes. *J. Phys. Chem. Lett.* **2020**, *11*, 3111–3115.

[5] Jia, S. Q.; Tang, H. D.; Ma, J. R.; Ding, S. H.; Qu, X. W.; Xu, B.; Wu, Z. H.; Li, G. Y.; Liu, P.; Wang, K. et al. High performance inkjet-printed quantum-dot light-emitting diodes with high operational stability. *Adv. Opt. Mater.* **2021**, *9*, 2101069.

[6] Shirasaki, Y.; Supran, G. J.; Bawendi, M. G.; Bulović, V. Emergence of colloidal quantum-dot light-emitting technologies. *Nat. Photonics* **2013**, *7*, 13–23.

[7] Shen, H. B.; Lin, Q. L.; Cao, W. R.; Yang, C. C.; Shewmon, N. T.; Wang, H. Z.; Niu, J. Z.; Li, L. S.; Xue, J. G. Efficient and long-lifetime full-color light-emitting diodes using high luminescence quantum yield thick-shell quantum dots. *Nanoscale* **2017**, *9*,

13583–13591.
[8] Chen, S.; Cao, W. R.; Liu, T. L.; Tsang, S. W.; Yang, Y. X.; Yan, X. L.; Qian, L. On the degradation mechanisms of quantum-dot light-emitting diodes. *Nat. Commun.* **2019**, *10*, 765.
[9] Wang, F. F.; Hua, Q. Z.; Lin, Q. L.; Zhang, F. J.; Chen, F.; Zhang, H. M.; Zhu, X. X.; Xue, X. L.; Xu, X. P.; Shen, H. B. et al. High-performance blue quantum-dot light-emitting diodes by alleviating electron trapping. *Adv. Opt. Mater.* **2022**, *10*, 2200319.
[10] Chrzanowski, M.; Zatryb, G.; Sitarek, P.; Podhorodecki, A. Effect of air exposure of ZnMgO nanoparticle electron transport layer on efficiency of quantum-dot light-emitting diodes. *ACS Appl. Mater. Interfaces* **2021**, *13*, 20305–20312.
[11] Wang, L. X.; Tang, C. G.; Tan, Z. S.; Phua, H. Y.; Chen, J.; Lei, W.; Png, R. Q.; Chua, L. L.; Ho, P. K. H. Double-type-I charge-injection heterostructure for quantum-dot light-emitting diodes. *Mater. Horiz.* **2022**, *9*, 2147–2159.
[12] Kong, L. M.; Wu, J. L.; Li, Y. G.; Cao, F.; Wang, F. J.; Wu, Q. Q.; Shen, P. Y.; Zhang, C. X.; Luo, Y.; Wang, L. et al. Light-emitting field-effect transistors with EQE over 20% enabled by a dielectric-quantum dots-dielectric sandwich structure. *Sci. Bull.* **2022**, *67*, 529–536.
[13] Wu, Q. Q.; Gong, X. W.; Zhao, D. W.; Zhao, Y. B.; Cao, F.; Wang, H. R.; Wang, S.; Zhang, J. H.; Quintero-Bermudez, R.; Sargent, E. H. et al. Efficient tandem quantum-dot LEDs enabled by an inorganic semiconductor-metal-dielectric interconnecting layer stack. *Adv. Mater.* **2022**, *34*, 2108150.
[14] Wu, Q. Q.; Cao, F.; Wang, S.; Wang, Y. M.; Sun, Z. J.; Feng, J. W.; Liu, Y.; Wang, L.; Cao, Q.; Li, Y. G. et al. Quasi-shell-growth strategy achieves stable and efficient green InP quantum dot light-emitting diodes. *Adv. Sci.* **2022**, *9*, 2200959.
[15] Cao, W. R.; Xiang, C. Y.; Yang, Y. X.; Chen, Q. Chen, L. W.; Yan, X. L.; Qian, L. Highly stable QLEDs with improved hole injection via quantum dot structure tailoring. *Nat. Commun.* **2018**, *9*, 2608.
[16] Chen, D. S.; Chen, D.; Dai, X. L.; Zhang, Z. X.; Lin, J.; Deng, Y. Z.; Hao, Y. L.; Zhang, C.; Zhu, H. M.; Gao, F. et al. Shelf-stable quantum-dot light-emitting diodes with high operational performance. *Adv. Mater.* **2020**, *32*, 2006178.
[17] Chen, Z. N.; Su, Q.; Qin, Z. Y.; Chen, S. M. Effect and mechanism of encapsulation on aging characteristics of quantum-dot light-emitting diodes. *Nano Res.* **2021**, *14*, 320–327.
[18] Peng, H.; Yu, A. R.; Liu, S. B.; He, Y.; Chen, X. Q.; Hu, Y. M.; Zeng, Q.; Qin, J. J.; Tang, Y. J.; Xuxie, H. N. et al. Coulomb effect induced intrinsic degradation in OLED. *Org. Electron.* **2019**, *65*, 370–374.
[19] Hu, C.; Wang, Q.; Bai, S.; Xu, M.; He, D. Y.; Lyu, D. Y.; Qi, J. The effect of oxygen vacancy on switching mechanism of ZnO resistive switching memory. *Appl. Phys. Lett.* **2017**, *110*, 073501.
[20] Chen, J. Y.; Hsin, C. L.; Huang, C. W.; Chiu, C. H.; Huang, Y. T.; Lin, S. J.; Wu, W. W.; Chen, L. J. Dynamic evolution of conducting nanofilament in resistive switching memories. *Nano Lett.* **2013**, *13*, 3671–3677.
[21] Chang, W. Y.; Huang, H. W.; Wang, W. T.; Hou, C. H.; Chueh, Y. L.; He, J. H. High uniformity of resistive switching characteristics in a Cr/ZnO/Pt device. *J. Electrochem. Soc.* **2012**, *159*, G29–G32.
[22] Xu, N.; Liu, L. F.; Sun, X.; Liu, X. Y.; Han, D. D.; Wang, Y.; Han, R. Q.; Kang, J. F.; Yu, B. Characteristics and mechanism of conduction/set process in TiN/ZnO/Pt resistance switching random-access memories. *Appl. Phys. Lett.* **2008**, *92*, 232112.
[23] Simanjuntak, F. M.; Ohno, T.; Samukawa, S. Neutral oxygen beam treated ZnO-based resistive switching memory device. *ACS Appl. Electron. Mater.* **2019**, *1*, 18–24.
[24] Lee, H.; Jeong, B. G.; Bae, W. K.; Lee, D. C.; Lim, J. Surface state-induced barrierless carrier injection in quantum dot electroluminescent devices. *Nat. Commun.* **2021**, *12*, 5669.
[25] Chang, J. H.; Park, P.; Jung, H.; Jeong, B. G.; Hahm, D.; Nagamine, G.; Ko, J.; Cho, J.; Padilha, L. A.; Lee, D. C. et al. Unraveling the origin of operational instability of quantum dot based light-emitting diodes. *ACS Nano* **2018**, *12*, 10231–10239.
[26] Lu, J. F.; Xu, C. X.; Dai, J.; Li, J. T.; Wang, Y. Y.; Lin, Y.; Li, P. L. Improved UV photoresponse of ZnO nanorod arrays by resonant coupling with surface plasmons of Al nanoparticles. *Nanoscale* **2015**, *7*, 3396–3403.
[27] Zhou, H.; Alves, H.; Hofmann, D. M.; Kriegseis, W.; Meyer, B. K.; Kaczmarczyk, G.; Hoffmann, A. Behind the weak excitonic emission of ZnO quantum dots: ZnO/Zn$(OH)_2$ core-shell structure. *Appl. Phys. Lett.* **2002**, *80*, 210–212.
[28] Nair, S. V.; Sinha, S.; Rustagi, K. C. Quantum size effects in spherical semiconductor microcrystals. *Phys. Rev. B* **1987**, *35*, 4098–4101.
[29] Zhang, W. J.; Chen, X. T.; Ma, Y. H.; Xu, Z. W.; Wu, L. J.; Yang, Y. X.; Tsang, S. W.; Chen, S. Positive aging effect of ZnO nanoparticles induced by surface stabilization. *J. Phys. Chem. Lett.* **2020**, *11*, 5863–5870.
[30] Ding, S. H.; Wu, Z. H.; Qu, X. W.; Tang, H. D.; Wang, K.; Xu, B.; Sun, X. W. Impact of the resistive switching effects in ZnMgO electron transport layer on the aging characteristics of quantum dot light-emitting diodes. *Appl. Phys. Lett.* **2020**, *117*, 093501.